Review Article

Yuqing Dong, Ka-Wai Yeung, Chak-Yin Tang*, Wing-Cheung Law, Gary Chi-Pong Tsui, and Xiaolin Xie

Development of ionic liquid-based electroactive polymer composites using nanotechnology

https://doi.org/10.1515/ntrev-2021-0009
received February 26, 2021; accepted March 13, 2021

Abstract: This review is intended to provide an overview of the design and fabrication of ionic liquid-based ionic electroactive polymer (IL-iEAP) transducers for advanced applications in biological and electronic fields. The iEAP is a class of smart materials that can perform sensing or actuating functions by controlling the movement of cations and anions in the active layer. This type of material can deform under low voltage stimulation and generate electrical signals when undergoing mechanical deformation because of ion redistribution. Numerous research attention has been focused on studying the deformation mechanisms and the potential for actuation, sensing, and energy harvesting applications. Compared to the traditional water-based iEAP, the non-volatile IL-iEAP delivers a wider electrochemical window and a more stable actuation performance. In this paper, the classification of iEAP with different actuation mechanisms is first outlined, followed by introducing various preparation methods including nanotechnology for IL-iEAPs, and discussing the key factors governing their actuation performance. In addition, the advanced functions of IL-iEAP in actuating and sensing, especially self-sensing in bionics and electromechanical equipment applications, are reviewed. Finally, novel nanotechnologies used for fabricating IL-iEAPs and the prospects of their microelectromechanical system (MEMS) applications are discussed.

Keywords: ionic liquid, electroactive polymer, smart materials

*** Corresponding author: Chak-Yin Tang,** Department of Industrial and Systems Engineering, The Hong Kong Polytechnic University, Hung Hom, Kowloon, Hong Kong, China, e-mail: cy.tang@polyu.edu.hk, tel: +852-2766-6608, fax: +852-2362-5267
Yuqing Dong, Ka-Wai Yeung, Wing-Cheung Law, Gary Chi-Pong Tsui: Department of Industrial and Systems Engineering, The Hong Kong Polytechnic University, Hung Hom, Kowloon, Hong Kong, China
Xiaolin Xie: School of Chemistry and Chemical Engineering, Huazhong University of Science and Technology, Wuhan, Hubei 430074, China

1 Introduction

Soft actuating polymers are smart materials that exhibit mechanical deformation in response to environmental physical or chemical stimuli. Compared with conventional hard actuators, such as piezoelectric ceramics or metallic materials, soft actuators possess the advantages of good flexibility, fast response, lightweight, and low power consumption and low cost [1–4]. Among various types of polymer-based actuators, electroactive polymers (EAPs) [5–8] are promising candidates in the fields of prosthetics [9], soft robotics [10,11], and biomedicine [12,13] because of their intrinsic properties that include a broad actuation voltage range (1 V to 5 kV) and a wide range of working mediums (*e.g.*, salt solutions and open air). In recent years, it has been reported that EAPs are suitable for aerospace applications because of good adaptability to operate in extreme temperature and radiation conditions [14].

EAPs are polymer composites that perform reversible physical deformation under electric stimuli [15]. The first discovery of EAP can be traced back to the 1880s [16], where a simple design of elastomer actuator was developed, and its actuation was achieved by spraying electric charges on the surface of rubber. Because polyvinylidene fluoride (PVDF) with a better piezoelectric property has been reported, researchers began to focus on ferroelectric polymer systems, which enabled the rapid development of EAP in the early 1970s [17] with faster response rate and higher actuation efficiency. Generally, EAP can be classified as electronic or ionic. EAPs actuated under voltage higher than 3 kV are known as the electronic class (eEAP). These actuators, such as dielectric elastomers, demonstrate a reversible expansion and contraction because of the compression of Maxwell's electrostatic force between the two electrodes [18,19]. On the contrary, ionic type

EAPs (iEAPs) [20] normally operate at a lower voltage (<20 V) as compared to eEAPs. Conventional actuation of iEAP usually requires a solvent medium, and the bending response greatly depends on the ambient humidity or the solvent concentration. Therefore, it is also called wet-iEAP. Compared to eEAP, the response of iEAP is usually slower but more flexible.

A variety of iEAPs with a low operating voltage, including ionic polymer-metal composite (IPMC) [21], conductive polymer (CP) [22], ionic polymer gel (IPG) [23], and carbon nanotube (CNT) composite paper [24], have been developed and used in the field of smart materials and biomimetics. They are multi-layer structured, consisting of a solid electrolyte layer sandwiched between two electrode layers. The typical structures, materials, and applications of iEAP are shown in Figure 1. The bending strain of iEAP is dependent on the modulus of the material and the actuation voltage [25]. iEAPs with low elastic modulus and relatively high driving voltage are conducive for achieving large deformation. However, this may compromise the cycle life, especially for the water-based IPMC because of the narrow electrochemical window of water. In addition, the electrode layers are also considered fragile for frequent bending. Moreover, the back-relaxation phenomena of iEAPs limit their applications as actuators because of the attenuated deflection under direct current (DC) [26,27]. While under a high frequency alternating current (AC), the bending strain of iEAP decreases exponentially compared with operating at low frequency. In the past 5 years, numerous novel iEAP-based composite materials have been developed to extend the application of iEAPs by overcoming the above-mentioned hurdles [28]. Among them, ionic liquid-based iEAPs (IL-iEAPs) show extraordinary actuation performance without compromising the cycle life or its unique feature of low actuation voltage. They have become a new research hotspot because of the properties of the wide electrochemical window, almost negligible vapor pressure, and high ionic conductivity, leading to the advantages of wider voltage range, better stability, and extended cycle life.

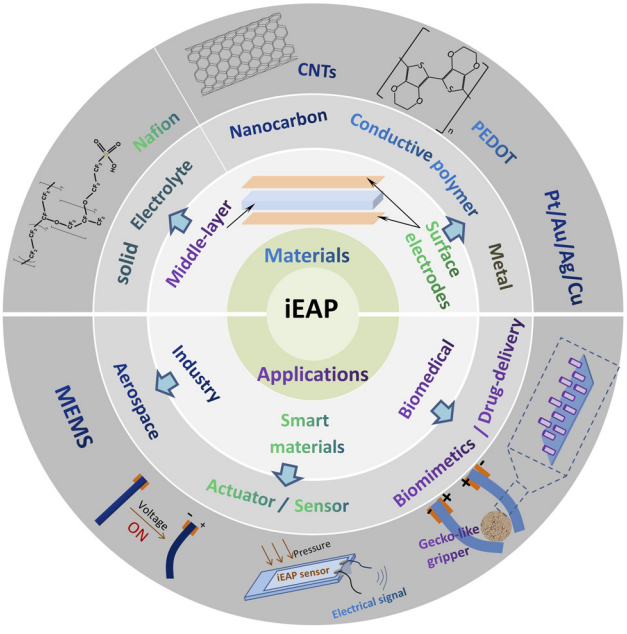

Figure 1: Overview of the materials' composition and applications of iEAP.

In this review paper, the fundamentals of IL-iEAP with a classic three-layer structure that can stably operate in the open air are first described. Then, three main types of IL-iEAPs, namely IPMC, CP, and bucky gel, and their bending mechanisms are introduced. In addition, the state-of-the-art technology for fabricating IL-iEAPs, including the fabrication of the electrode layer and IL-containing electrolyte layer, is presented. Nanotechnologies, such as self-assembly and magnetron sputtering, as well as the inclusion of nanomaterials, including CNTs and silver nanowires, are commonly applied for the fabrication of the electrode layers [6,15,20]. These can improve the conductivity of the electrode layer without compromising the mechanical properties of iEAP including the flexibility because of the ultra-thin thickness of electrodes. In addition, the contact area and interfacial bonding between the electrode layers and the electrolyte are enhanced through chemical self-assembly and forming intercalation structure [21]. Moreover, carbon nanomaterials are beneficial to enhance the bending response of iEAP because of their inherent electromechanical response when being used as electrode materials [24]. The main factors governing the bending performance and the actuation behavior of the IL-iEAPs are discussed. This is followed by reviewing the applications of IL-iEAPs in the field of biomimetic soft robots and biosensing. Finally, the future development of the fabrication technology and potential applications of these low voltage driven soft actuators is discussed.

2 Fundamentals of IL-iEAP

ILs are room temperature molten salts containing cations, anions, and neutral molecules. They have been used in various energy conversion applications and electroactive devices [29], serving as the ion source for producing solid electrolyte layers in iEAP. Some commonly used ILs are

Table 1: Commonly used ILs for iEAP

IL	Abbreviation	Cation	Anion	Ref.
1-Ethyl-3-methylimidazolium trifluoromethanesulfonate	EMIMOtf		$CF_3SO_3^-$	Almomani *et al.* [30]
1-Ethyl-3-methylimidazolium tetrafluoroborate	$EMIMBF_4$		BF_4^-	Guo *et al.* [31]
1-Ethyl-3-methylimidazolium Bromide	EMIMBr		Br^-	Kim *et al.* [32]
1-Ethyl-3-methylimidazolium bis(trifluoromethylsulfonyl) imide	EMITFSI		$N(CF_3SO_2)_2^-$	Woehling *et al.* [33]
1-Butyl 3-methylimidazolium chlorine	BMIMCl		Cl^-	Liu *et al.* [34]
1-Butyl-3-methylimidazolium hydrogen sulfate	BMIMHS		$(SO_3OH)^-$	Panwar *et al.* [35]
1-Butyl-3-methylimidazolium tetrafluoroborate	$BMIMBF_4$		BF_4^-	Montiel *et al.* [36]

listed in Table 1. IL-iEAP can be classified into IPMC, CP, and bucky gel, depending on the material used for the electrode layers. In these iEAPs, IL provides the source of ions with volume differences for achieving bending deformation. In bucky gel, IL serves as a dispersant and cross-linking agent for nanocarbon (*e.g.*, CNT). iEAPs with different electrode materials bend under different mechanisms. The actuation performance of IL-iEAPs, including response rate, degree of deflection, and cycle life, depends greatly on the electronic conductivity and durability of the electrode and the ionic conductivity of the electrolyte. In the following sections, the basics of different IL-iEAPs, including their development, structures, and actuation mechanisms, are presented.

2.1 IPMC

A typical IPMC consists of a commercially available ion exchange membrane (such as Nafion) with thin layer of noble metal (such as Pt, Au, and Ag) electrodes deposited on both sides [29,37]. The ion exchange membrane is fully swollen by water, providing channels for cations to freely flow inside. When IPMC is energized across its thickness, the hydrated cations move to the cathode and accumulate, leading to the expansion and bending of the cathode side towards the anode in a macroscopic view, as shown in Figure 2. This type of water-based IPMC is suitable as an actuator material. The high ionic conductivity of the electrolyte layer confers the advantages of fast response, large deformation, and low operating voltage. However, there are critical problems that may lead to the failure of IPMC. Several failure mechanisms of water-based IPMC studies have been reported [38–40]. For example, because of the narrow electrochemical stable window of water, electrolysis occurs at a voltage higher than 1.23 V [39]. This leads to the reduction of ion migration channels and ion mobility. Besides, the cracking of electrode caused by frequent bending results in water leakage and evaporation, which limits the cycle life of IPMC [40]. Moreover, it was reported that the density of the electrode cracks is related to the cation species in the electrolyte membrane [41]. A higher crack density was found in an IPMC sample containing smaller cations such as H^+ or Li^+.

Numerous methods have been developed to extend the cycle life of the water-based IPMC, such as optimizing the preparation process [42], using ethylene glycol or glycerin as solvents instead of water [43,44], doping hygroscopic nanoparticles to maintain the humidity [45], reinforcing the IPMC by a casting electrode protection layer [46], as well as coating the whole IPMC with an isolation layer [47]. Recently, Guo *et al.* [40] fabricated PEDOT-coated metal electrodes *via* electric grafting to compensate for the metal cracks caused by bending, and enduring testing indicated that its durability was extended to 83 min. However, these methods could only lead to limited improvement of cycle life of IPMC. The reinforcement by the additional layer might also have an adverse effect on the actuation performance of IPMC.

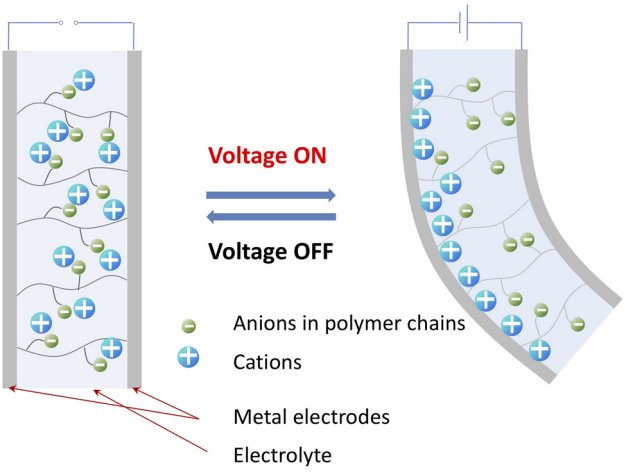

Figure 2: Actuation mechanism of IPMC.

Using non-volatile IL as the solvent in the electrolyte layer of IPMC can significantly improve the stability of the actuator in the open air [32]. The bending mechanism of IL-based IPMC is similar to the traditional water-based IPMC as shown in Figure 2. The accumulation of cation on the cathode and anion on the anode causes a volume difference between the two sides and results in bending. Liu *et al.* [34] characterized the depth profile of mobile ions in the ionomer membrane containing BMIMCl (1-butyl 3-methylimidazolium chlorine) sandwiched with two gold electrodes through the use of time-of-flight secondary ion mass spectrometry, confirming that the anions and cations gather near the anode and cathode, respectively. It is worth noting that the IL used in the electrolyte layer was not completely dissociated [48], and the anions and cations of IL showed different migration rates [49]. Therefore, the bending direction [50,51] and the degree of deflection [52] of IL-based IPMC were affected by the product difference of the ions migration quantity and their Van der Waals volume under the electric field. However, the back-relaxation still exists in IL-IPMC. Further, the response rate of IL-IPMC would be significantly slower than that of the water-based IPMC because IL shows lower mobility in electrolyte because of its high viscosity [53].

2.2 CP actuators

CPs, such as polypyrrole (PPy), polyaniline (PANI), and polythiophene, are organic semiconductors called organometallics [54]. CPs are more desirable as electrode materials in electronic devices owing to their flexibility and ease of handling as compared to metals [55–57]. Similar to the working principle of IPMC, when a voltage is applied between two CP electrodes, a bending motion can be produced toward one side of the electrode [22]. In the 1990s, the actuation of CP under an electric field was achieved by immersing the CP actuator in an electrolyte solution. The CP matrix in electrochemical oxidation or a reduction state was neutralized by ions implantation or de-intercalation, and the expansion and contraction of the actuator were achieved by the movement of the CP chain because of the mass transfer of ions [58,59]. In addition, CP actuators with linear actuation can be achieved by a tri-layer structure, in which an electrolyte layer is embedded in the CP [55]. The development of solid electrolytes allows CP actuators to deform in the open air. These dry CP actuators no longer require the environment humidity compared to wet ones [60].

In CP actuator systems, electrochemical oxidation and reduction of CP take place in the anode and cathode polymers, respectively. At the anode electrode, positive holes are generated within the CP chain and insertion of anions from the solid electrolyte may occur. In contrast, the negatively charged free electrons on the cathode lead to deintercalation of anions, favoring the directional migration of cations. Therefore, the driving motion of this tri-layer CP composite is a result of the synergistic effect between electrode electrochemical reaction and electrolyte ion migration [61], as shown in Figure 3.

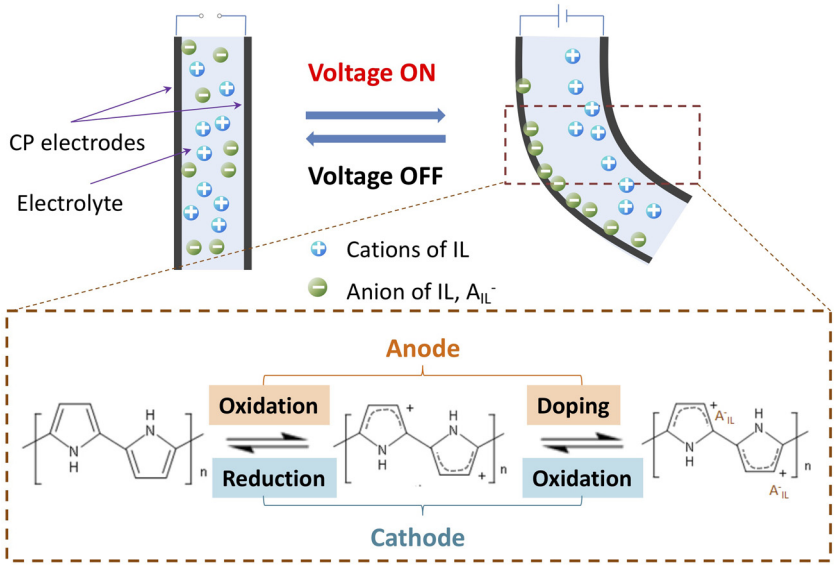

Figure 3: Actuation mechanism of CP actuator.

The activation of CP actuator mainly depends on minimum voltage triggering electrochemical insertion/de-intercalation of the electrodes. Therefore, a driving voltage as low as 1 V is sufficient to stimulate the CP actuator [62]. However, the influence of operating voltage on the bending performance such as direction and strain should be taken into consideration when designing the CP actuator [63,64]. For instance, a change of bending direction can be observed when the stimulation range is switched from 1 V/−0.55 V to 1 V/−1 V. This change results from the volume expansion of the different electrode caused by anions or cations [64].

2.3 Bucky gel

The third type of IL-iEAP is bucky gel, which functions like CP and serves as the electrode layer [24,65,66]. In a bucky gel actuator (BGA), IL is used in the electrode and electrolyte layer, as shown in Figure 4.

One typical bucky gel reported was a mixture of single-walled carbon tubes (SWCNTs) and ILs [67]. Nano carbon materials have been extensively studied and applied to various actuators or sensors [68–72]. In particular, CNT was widely used in actuator materials because of the excellent mechanical, electrical, electromagnetic, and opto-thermal properties [73–76]. In 1999, Baughman *et al.* [77] reported for the first time that an actuator made of two SWCNT sheets bonded by insulating glue exhibited bending behavior under a voltage of 1 V in sodium chloride solution. The bending mechanism was later explained as being because of the quantum chemical expansion [77], electrochemical double-layer charging [78], and Coulomb repulsion effect [79]. However, because of the high cost of SWCNTs sheets, the application of these actuators was limited. Besides, SWCNTs easily agglomerate and are difficult to disperse and process. Different techniques were developed to overcome these problems. Fukushima *et al.* [67] discovered that imidazole-based IL is a good dispersant for SWCNTs. The CNT bundles can be unwound and untangled by the cation–π interaction. In this work, the SWCNTs and ILs were ground in a mortar to form a physically cross-linked composite gel with good electronic and ionic conductivity. Later, Fukushima *et al.* [80] also reported the fabrication of tri-layer iEAP through layer-by-layer casting using SWCNTs/IL composited gel with PVDF glue. The actuation mechanism of the BGA is the combination of the volume change of CNT bucky gel, and the migration and accumulation of electrolyte ions near the electrode [81]. As both anode and cathode electrode layers show the same deformation direction, this leads to a synergistic bending effect in the BGA, and thus, a larger bending deformation can be achieved [66,82].

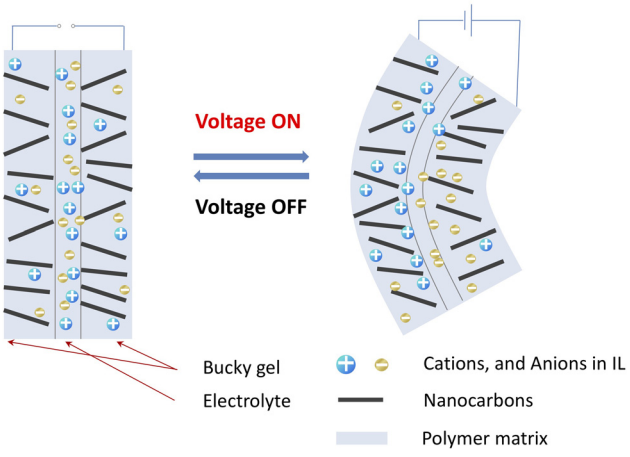

Figure 4: Actuation mechanism of BGA.

3 Preparation of dry iEAP containing IL

IL-iEAP is usually a three-layer strip composed of electrodes and a solid electrolyte, in which the electrodes play important roles in the actuation performance. In this section, we introduce the state-of-the-art preparation method of IL-iEAP, focusing on the synthesis and assembly for different electrodes by chemical and physical approaches. The common approaches for fabricating IL-iEAP are listed in Table 2.

3.1 Chemical approaches

The chemical approaches for deposition of electrodes on a solid electrolyte include electroless plating of metal and electropolymerization or *in situ* polymerization of CP. Generally, the electrodes are prepared from metal cations or monomers to the metal or polymer layer in chemical ways, as shown in Figure 5. After deposition of electrodes, the ions are loaded on the electrolyte layer by an impregnation process.

Electroless plating is a reduction process. The metal cations that enter the polymer matrix membrane through ion exchange are reduced to metal and deposited on the membrane surface to form thin electrode layers [41,53,90].

Table 2: Chemical and physical fabrication approaches of IL-iEAP

Categories	Methods	Material	Ref.
Chemical way	Electroless plating	Metal	Kim *et al.* [32]
Pros: strong interface bonding	Electropolymerization	PPy	Naficy *et al.* [83]
		PEDOT: PSS	
Cons: complex processing and time-consuming	*In situ* polymerization	PEDOT: PSS	Khmelnitskiy *et al.* [84]
		PANI	
Physical way	Spray coating	Metal powder	Terasawa [85]
Pros: simple processing and mass production		PEDOT: PSS	
Cons: weak interface bonding	Dip coating		Kim *et al.* [86]
	Spin coating		Hu *et al.* [87]
	Drip coating		Kotal *et al.* [88]
	Hot-pressing	Self-supporting film electrodes such as metal foil and bucky gel	Park *et al.* [46]
			Morozov *et al.* [89]

Generally, a semi-interpenetrating structure, which is formed between the metal electrodes and the ion exchange membrane, contributes to the enhancement of interface bonding and electrical conductivity. The tri-layer structure in IL-iEAP is obtained by immersing the sample in IL solution (usually >12 h) [32]. In this case, temperature is a key factor affecting the absorption rate because of the high viscosity and large molecular weight of ILs. According to the diffusion principle, a high immersion temperature is beneficial for the absorption of IL by the ion exchange

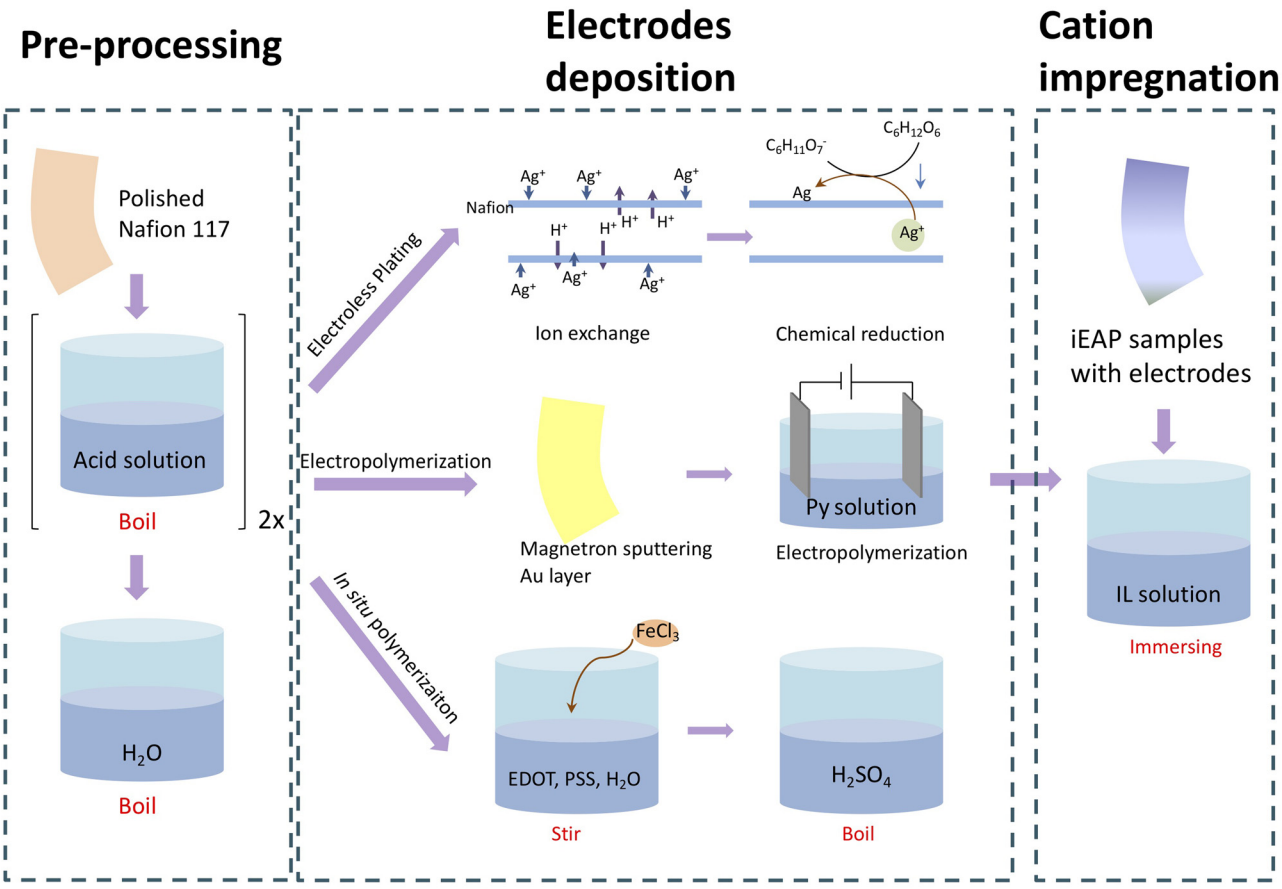

Figure 5: Schematic for the preparation IL-iEAP through chemical methods.

membrane [91]. However, a high-volume percentage of solvents in the swollen membrane will cause cracking of metal electrode layers, leading to the loss of the surface conductivity. For instance, the surface resistance of the Au electrode was increased by six orders of magnitude after IL absorption [92].

The conductivity of polymer electrodes coated by electropolymerization or *in situ* polymerization are not affected by the same IL absorption process because of its excellent flexibility [83]. Electropolymerization is commonly used to prepare PPy electrodes. Normally, an electrolyte membrane made of polymer film, such as PVDF and Nafion, sputtered with a thin layer of (<30 nm) gold [93] or platinum [60] metal on its surface is used for the electropolymerization. By immersing the membrane into a pyrrole monomer solution, PPy is deposited on the metal surface to form uniform CP layers under a constant current. Besides, poly(3,4-ethylenedioxythiophene) (PEDOT) is used to form a uniform layer on the surface of the electrolyte membrane *via in situ* polymerization [94]. This electrode film is more chemically stable because the chemical active position in the five-membered ring of PEDOT is modified and inactivated by oxygen [95]. Although the IL-iEAP prepared by chemical means shows excellent interface bonding property, it is still a challenge to control the morphology and thickness of electrodes. Therefore, physical methods have attracted more research interest because it is more accessible in fabricating electrodes with controllable shape and cost.

3.2 Physical approaches

The physical approaches involve various coating methods (for metal powder or soluble CP) and hot-pressing (for self-supporting electrode layers such as metal foil or bucky gel), as shown in Figure 6. Differing from chemical processing, the electrolyte layer loaded with IL is usually fabricated before the electrode is assembled. Therefore, this can avoid cracking of the electrode layers caused by the IL solution swelling process.

Akle *et al.* [92] successively sprayed metal powder dispersions and metal oxide powder on the surface of the IL electrolyte membrane to prepare the electrode

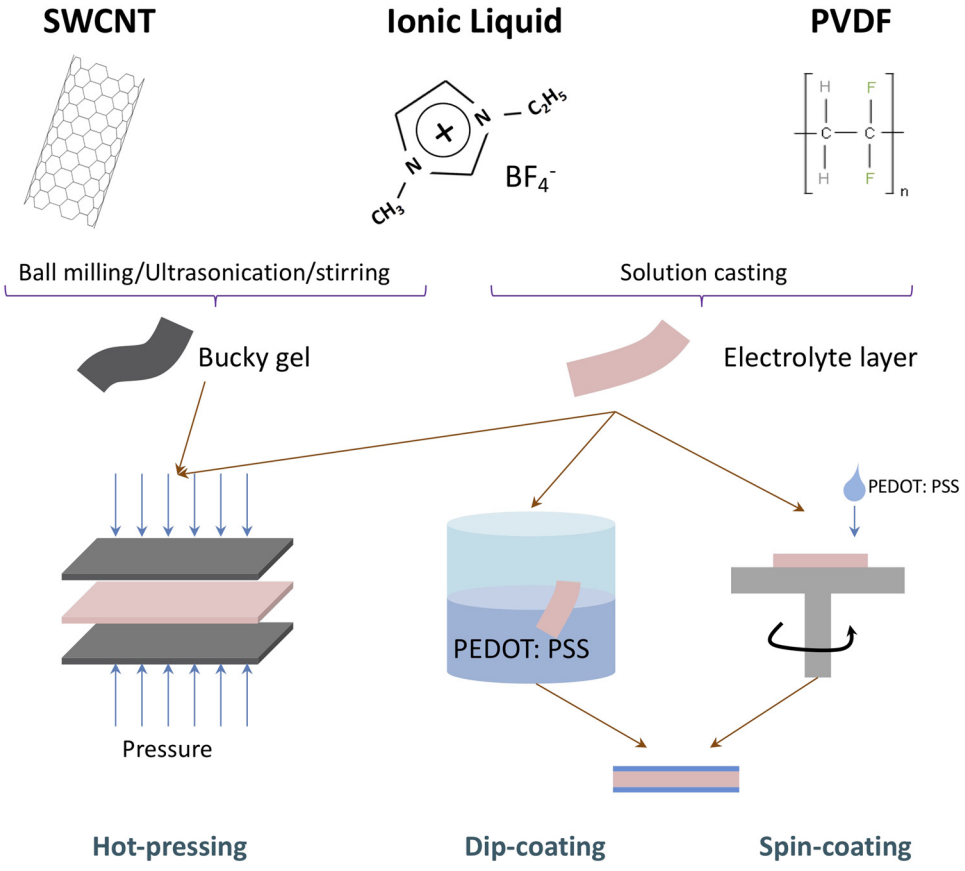

Figure 6: Typical physical approaches for preparing IL-iEAP.

layer with a high specific surface area, which is beneficial for increasing the output strain. The IL-iEAP sample was finally produced by hot-pressing with two gold foils to further reduce the electrode resistance. Lin *et al.* [96] reported a simple process to prepare IL-iEAP by hot-pressing gold electrodes directly on a commercial Aquivion membrane impregnated with IL. It is worth noting that poor adhesion between the electrolyte and electrode occurs when the concentration of IL in the electrolyte is lower than 23.07 wt% [97]. The same processing was applied by Almomani *et al.* [30] to study the temperature dependence of the electromechanical properties of IL-iEAP containing EMIMOtf (1-ethyl-3-methylimidazolium trifluoromethanesulfonate). The hot-pressing method is also suitable for self-supporting electrodes including metal nanowires composites [46] and bucky gel [66,82,89,98]. The subsequent spin-coating with water-soluble poly(3,4-ethylenedioxythiophene): poly(styrene sulfonate) (PEDOT: PSS) works as a protective layer for reducing the sheet resistance of electrodes, and improving the response rate and bending amplitude [46]. Nevertheless, attention should be paid to the control of the hot-pressing temperature to prevent the electrolyte membrane from melting.

Other physical approaches for assembling IL-iEAP include various coating methods for PEDOT: PSS electrodes. Good interface properties between the electrode layer and the electrolyte membrane are crucial for achieving excellent deformation and durability of the actuator. It was reported that better compatibility between the electrolyte layer and electrode can be achieved by adding DMSO into the PEDOT: PSS aqueous solution [99,100]. In addition, the porous structure of the electrolyte membrane favors the electrode material adsorption. A freeze-dried bacterial cellulose membrane with a 3D porous network showed strong adhesion with the dip coated PEDOT: PSS electrodes [86]. When a hydrophobic polymer, such as PVDF, was used as the electrolyte layer, applying surface hydrophilic treatment before electrodes coating was proven to be a useful method for improving the interface strength [101].

In recent years, novel technologies such as ink-jet printing have been applied to the preparation of CP electrode layers, providing new possibilities for the mass production of IL-iEAP. Põldsalu *et al.* [102] used a low concentration (0.6–1.2 wt%) PEDOT: PSS ink to print on the polymer film substrate through a precision printing platform equipped with a drop-on-demand printhead. Generation of the electrode film was achieved by solvent evaporation of the ink. A three-layer iEAP sample with a thickness of only 12.7 microns was produced by repeating the ink-jet printing process for the other side of polymer substrate. Printing methods are also commonly used for the fabrication of BGAs. The bending deformation is related to the thickness of the electrode layers, which can be adjusted by the number of printing layers. Mukai *et al.* [82] reported that the BGA with five-layer electrodes performs larger bending strain (~0.4%) than the single-layer actuator (~0.3%).

3.3 Hybrid approach

There are advantages and disadvantages in the chemical and physical approaches for preparing IL-iEAP. Good interface bonding helps to enhance the electrical conductivity along the thickness and length directions of the electrode layer, thereby enhancing the movement of ions. In addition, the electrode is not easily detached from the surface of the electrolyte membrane during the bending motion. The shape and thickness of the electrode are also important factors affecting the bending performance, especially for BGAs. Therefore, by combining the individual advantages of the two approaches, a hybrid method is an effective compromise for preparing iEAP composite electrodes. It has been reported that iEAP with chemically deposited graphene electrodes and a protective PEDOT: PSS layer can maintain the original conductivity and the response level, even after the sample placed in an open environment for 30 days [103].

4 Actuation performance of IL-iEAP

In this section, the governing factors, such as the properties of the electrolyte and electrode layers, on the actuation performance of IL-iEAP are analyzed. The actuation performance of IL-iEAP includes response rate, saturation time, deflection angle or tip displacement, and bending strain. This section also presents the causes and the solutions for back-relaxation in IL-IPMC under DC stimulation.

4.1 IPMC

The bending behavior of IPMC originates from the volume difference near the electrode region because of the ion migration and accumulation under an external electric potential. However, introducing highly viscous ILs into the IPMC may impede the response rate [104], as a consequence of the high molecular weight of the ILs and the

low ions diffusion coefficient [105]. This problem can be addressed by selecting suitable ILs with lower molecular weight. Kim *et al.* [32] conducted a comparative experiment using different ILs to investigate the effect of the molecular weight of ILs on the IPMC response rate. It was found that the IL-IPMC doped by EMIMBr (1-ethyl-3-methylimidazolium Bromide) with the lowest molecular weight achieved the highest response rate of 0.73 mm s^{-1}, under AC voltage stimulation (±3 V, 0.1 Hz). The response rate is comparable to that of the water-based IPMC, with only a difference of 0.02 mm s^{-1}. ILs with higher molecular weight may impede the bending motion and extend the saturation time of the actuator because of the low diffusion coefficient. Guo *et al.* [31] reported that the $EMIMBF_4$-IPMC with high molecular weight demonstrated nearly ten times the saturation time compared to the Li^+ containing water-based sample. Consequently, the authors suggested an innovative approach to improve the bending performance by providing an additional channel to facilitate ion migration. IL-IPMCs with interconnected micro/nano-porous structure were produced by the template method for this purpose and the IL-IPMCs achieved a faster and larger bending deformation [31]. A maximum bending angle of 75.4° was achieved under AC stimulation (±15 V, 0.1 Hz), which was only 5.7° smaller than that of the water-based inorganic salt sample [31].

The bending performance of IPMC may also be affected by the ionic conductivity of the electrolyte layer. Generally, the migration behavior of ions in the electrolyte layer can be explained by electrophoresis [106] or electroosmosis [107]. Whether it is in water-based or IL-based IPMC, the electromechanical performance is always a positive correlation with the ionic conductivity of the electrolyte layer. Therefore, it is believed that the ionic conductivity of the electrolyte layer is an effective basis for predicting and evaluating the electromechanical performance of IPMC [31,53,92,108]. Further, it was confirmed that the operating temperature has direct implication on the electrolyte ionic conductivity and electromechanical properties [30]. The ionic conductivity of the electrolyte layer and the actuation curvature of IPMC decreased with increase in environmental temperature. When the temperature was higher than 70°C, no obvious curvature was observed. By analyzing the electrochemical behavior of IPMC at different temperatures, it was found that the actuator was physically or chemically degraded at high temperatures. Lin *et al.* [96] reported an investigation of the electric charge dynamics of the polymer/IL blend membrane, and the results indicated that reducing the thickness of the electrolyte layer of IPMC is conducive to improve the actuation rate. In addition, the durability of IL-IPMC in the open air depends on the electrolytic stability of ILs, which is mainly affected by the environmental conditions, such as temperature.

The electrical properties of the electrode layer constitute another important factor affecting the actuation performance of IPMC [109–111]. Akle *et al.* [92] suggested that the bending strain is highly attributed to the charge accumulation at the polymer-electrode interface in the ionic polymer actuator. A larger actuation strain can be achieved through a higher capacity of the iEAP which benefits from the increasing surface-to-volume ratio of metal particles in the electrodes. At 1 Hz, the actuation strain was up to 0.82% (2 V) and 2.44% (4 V). Park *et al.* [46] reduced the surface resistance of the electrode to 160 mΩ sq^{-1} by spin-coating the PEDOT: PSS on a silver nanowire electrode. The response rate of IPMC was 34.83% faster than the sample without the CP.

The performance of IL-based IPMC may be affected by the displacement attenuation, which is usually named as back-relaxation, under DC stimulation. The typical manifestation of backward relaxation is that the actuator initially bends toward the anode and then deflects slowly toward the cathode over time, and even returns its original position or bends slowly toward the cathode. It is generally believed that the back-relaxation of IL-IPMC is caused by the different migration rates of zwitterions in the electrolyte membrane [49]. Therefore, improving the mechanical coupling [112] of the ions and electrolyte polymer such as PVDF is advantageous for inhibiting the back-relaxation. An electrolyte layer with single-ion migration was successfully synthesized using sulfonated block copolymer containing zwitterionic [28]. This actuator has shown a large deflection displacement of 2 mm under a low voltage and high frequency (±1 V, 10 Hz), with no back-relaxation in 200 s. Another explanation for the back-relaxation behavior is the decomposition of impurities (usually water) in the IL under constant voltage [53]. ILs with smaller cations may lead to higher water absorption, which cause back-relaxation because of the electrolysis of water. Therefore, controlling the size of cations and the relative humidity of the working environment were confirmed as effective approaches to inhibit back-relaxation of IL-IPMC [41].

The conductivity, stability, and interface characteristics of the electrolyte and electrode layers have great influence on the actuation performance of IL-IPMC. Although numerous efforts have been devoted to enhancing the actuation performance, it is still challenging to produce IL-IPMC with rapid, stable, and controllable deformation, by improving the properties of electrode and electrolyte. In

addition, the mechanism for improving the response rate of IL-IPMC by coating a CP [40] on the surface of metal electrodes is still under investigation.

4.2 CP

The electromechanical actuation performance of the CP actuator is mainly based on the volume change caused by the oxidation/reduction of the electrode layers [113]. Thus, studies on improving the actuation performance of CP actuator are mostly focused on the electrochemical properties of the electrode materials [114]. The electrode layer with higher conductivity [115] is more beneficial to its electrochemical oxidation response. For example, PEDOT: PSS, which possesses a low energy band gap and stable p-doped state, widely serves as a conductive material in electronic devices, including CP actuator [88]. Besides, flexible PEDOT: PSS film with higher conductivity can be obtained by adding surfactants or organic solvents to reduce the surface energy [46,116]. With the use of H_2SO_4 treatment, the highest conductivity (4,380 S cm^{-1}) of PEDOT: PSS film (thickness 100 nm) was obtained [117]. Põldsalu *et al.* [106] reported the ink-jet printing PEDOT: PSS electrodes on the EMIMTFSI/PVDF electrolyte membrane for fabricating a CP actuator. This actuator demonstrated a bending strain of 0.13% (under ±0.6 V, 0.0025 Hz) in the open air. Terasawa [85] prepared a CP actuator consisting of a PDMS/EMIMOtf electrolyte with spray coated PEDOT: PSS electrode, manifesting a large strain of 0.9% (under ±2 V, 0.05 Hz).

Another important factor affecting the bending strain of the CP actuator is the interface resistance between the electrolyte layer and CP electrodes. Electrodes fabricated *via* the chemical approaches show a low interfacial resistance that facilitates a larger deformation of CP actuators. Khmelnistskiy *et al.* [94] reported that an actuator with PEDOT: PSS electrodes coated by *in situ* polymerization shows a maximum deflection as large as 11 mm, compared to displacement of less than 1 mm of a drop-coating sample under the same actuation condition (5 V DC). For the CP actuator prepared by chemical approaches, the morphological characteristics of the electrodes also affect the bending performance. For instance, the PPy actuator with finer porous morphology electrodes showed a maximum tip displacement of 25 mm, which was 31.75% higher than for the PEDOT actuator [118]. In addition, applying PPy nanomaterials in the electrolyte layer is also effective in enhancing the interfacial bonding. *Khan et al.* [119] fabricated a PPy-based electrolyte film with PPy nanoparticles, which was synthesized by adjusting the dosage of the reducing agent during electropolymerization, to provide an additional support to the electrode layer. This CP actuator exhibited a maximum tip displacement of 9.85 mm under 2 V DC.

Generally, the unmodified CP shows low electrical conductivity under a reduced state, which limits the bending strain of the CP actuator [120]. This initiated the development of CP composite electrodes by doping with nanocarbon [20,121] or IL [122]. For instance, the IL-iEAP with PEDOT: PSS composite electrodes doped with acidified multi-walled carbon tubes (MWCNTs) showed faster and larger strain (0.64%). This actuator can maintain a rapid strain rate of 8.83% s^{-1}, even at a high frequency of 10 Hz, and the strain only lost ~0.06% even after 100,000 cycles [123].

4.3 Bucky gel

BGAs usually perform fast and large bending deformations that are highly dependent on the voltage frequency. Fukushima *et al.* [80] produced a first-generation BGA containing 13 wt% of SWCNT that exhibited excellent performance with a strain of 0.9% under ±3.5 V, 0.01 Hz. However, it was found that the actuation strain of the BGA deteriorated rapidly as the frequency of the square wave voltage increased. At a frequency of 10 Hz, a very small deflection (<0.05 mm) was recorded. The early design of the BGA exhibited the highest bending strain at a frequency lower than 0.05 Hz [81]. For example, Mukai *et al.* [82] studied the relationship between bending strain and stimulation frequency of a BGA, fabricated with two ultrathick (>0.23 mm) bucky gel layers by hot-pressing. The largest bending strain of 0.95% was achieved under ±2.5 V, 0.01 Hz. When the frequency was reduced to 0.005 Hz, the strain reached up to 1.9%. Moreover, Takeuchi *et al.* [81,124] successfully simulated the frequency dependence of various BGAs in electromechanical response through electrochemical kinetic models, showing that the frequency dependence of the actuation strain can be mainly attributed to the ionic conductivity of ILs and the content of SWCNTs in the electrode layers. In addition, a linear relationship between the bending strain of the actuator and its real capacitance at a frequency lower than 1 Hz has been reported [125]. In addition, the capacitance showed a positive correlation with the SWCNT concentration.

The second-generation bucky gel [98] was fabricated by introducing 50 wt% super-growth single-walled CNT (SG-SWCNT with millimeter in length), resulting in an

enhanced electrical conductivity (169 S cm^{-1}) of the electrode layer. This BGA showed an order of magnitude faster response rate (2.28% s^{-1}) than the first-generation under ±2.5 V, 1 Hz. Besides, the tip displacement was maintained even after more than 10,000 cycles. When the voltage frequency was increased from 1 to 10 Hz, the displacement was only reduced by less than 20%. Moreover, this BGA can work at 100 Hz. Similarly, Biso *et al.* [126] chemically modified CNT with diamine to obtain the cross-linked SG-SWCNT and fabricated a new BGA with less concentration of SWCNT (19 wt%) in the bucky gel. However, the conductivity of this bucky gel (1.7 S cm^{-1}) was much lower than that of the SG-SWCNT/IL (169 S cm^{-1}) as mentioned above. The bending strain of this BGA was less than 1% at 1 Hz and decreased by two orders of magnitude at 100 Hz. The electrical performance of the electrode showed a great influence on the actuation performance of iEAP. For example, a tri-layer actuator with self-supporting SWCNT electrodes and chitosan/$EMIMBF_4$ electrolyte demonstrated a fast response time (only 19 ms), as well as the actuation strain (9% s^{-1}), which far exceeded the second-generation BGA at 1 Hz [127]. This was because of the unique hierarchical structure of the self-supporting SWCNT electrodes with high electrical conductivity of 2,000 S cm^{-1}.

The high cost of SWCNTs for preparing bucky gel electrodes has switched interest to other carbon materials, such as MWCNTs [128], carbide-derived carbon [129], graphite [97], vapor grown carbon fiber [130], and cellulose nanofibers [131]. The structural characteristics of the BG electrodes may also affect the performance of the actuators. For instance, it was found that the high porosity of the carbon materials is advantageous for enhancing the performance of the actuator because of the large specific surface area. Moreover, it was reported that the interface contact between the electrolyte and the electrodes can be improved by adding a metal oxide nanolayer [132]. This also increases the ion diffusion channel and leads to a fast response (8.31% s^{-1}) of the actuator.

The actuation performance of BGA is related not only to the electrode carbon material but also to the electrolyte layer. It has been proven that the addition of an ionic polymer is favorable for improving the bending strain of the PVDF-HFP based BGA [133]. The interconnected porous structure of the electrolyte also facilitates the directional migration of ions. Morozov *et al.* [66] used a microporous PVDF membrane to prepare the electrolyte layer by absorbing IL directly. The maximum strain of this BGA can reach up to 1.35%. However, only limited research on the electrolyte layer has been conducted because of the restriction of the film thickness of 20–30 μm. Moreover, it is also challenging to predict the ionic conductivity and ion mobility of solid electrolyte by only studying the electrical properties of pristine IL [50].

In addition, although iEAP exhibits considerable bending response to a low voltage, the standards used to evaluate the bending deformation are not constant, which means that it is difficult to conduct a rational comparison for the actuation performance among iEAPs in different composite systems and sizes. Commonly used evaluation variables such as deflection angle, tip displacement, and curvature would show large deviations because of the differences in sample length and measurement position. Bending strain seems to be a reasonable physical quantity to describe the bending actuation of iEAPs. There are several methods to determine the bending strain of iEAPs. For example, Terasawa [85] stated the relationship between radius of curvature R and thickness with the bending strain ε as in the following equation:

$$\varepsilon = \frac{d}{R} = \frac{2d\delta}{L^2 + \delta^2},$$

where d is the thickness, δ is the tip deflection, and L is the effective length of the iEAP sample. This equation is derived with several assumptions: (i) the strain of the sample is uniform, along the plane parallel to the interlayer junction, and both the electrode and the electrolyte layer are isotropic elastomers; (ii) the bending section of the sample is still a plane; (iii) the elastic modulus change of the sample is negligible; and (iv) the change in sample thickness is much smaller than the change along its side length.

Fukushima *et al.* [80] derived the relationship between radius of curvature, modulus, and strain by assuming that the bending moment of the iEAP sample section and the elongation of the iEAP are both zero. Therefore, the following relationships can be established:

$$\varepsilon = \frac{\frac{2}{3}E_2\left(\frac{3}{4}h_1^2h_2 + \frac{3}{2}h_1h_2^2 + h_2^3\right) + \frac{1}{12}E_1h_1^3}{R \times [E_2(h_1h_2 + h_2^2)]},$$

where E_1 and E_2 are Young's moduli of the electrolyte and electrode layers with thicknesses of h_1 and h_2.

However, because the electrode conductivity of iEAP generally exhibits attenuation along its length, the distribution of ions and solvents inside the iEAP is not uniform, resulting in uneven and nonlinear bending deformation of the iEAP. Therefore, analyzing the angular deflection per unit length of an iEAP could be a more suitable way to evaluate the bending actuation of iEAPs.

5 Applications of IL-iEAP

IL-iEAP can be used for manufacturing biomimetic actuators including mechanical bats [134], gecko-like synthetic rubber [135], and worm robot [136], because of its stable actuation performance in the open air. In particular, a gripper is an essential part of bionic components with the simplest structure, and the gripping motion can be achieved by the opposite bending of the IL-iEAP actuators. A gripper system assembled by two CP actuators was reported to carry an object with approximately 50 times its mass under a voltage of 1.5 V [119]. Another iEAP soft gripper mimicked the micro-structure of gecko feet and was able to grasp objects with various surface features [137]. Other micro-controlled electromechanical actuators such as Braille displays [138], miniature autofocus lenses [139], and microfluidic valves [140] have also been reported. Besides, it is necessary to address the issues of biocompatibility, biological toxicity, and degradability of the actuator when iEAP is applied in the field of biomedicine [63,141–143]. Encapsulation [144] has been proven to be an effective method to develop biocompatible IL-iEAP actuators. However, this additional encapsulation layer increased the deformation resistance, thereby causing adverse effects on the actuation performance [142].

The IL-iEAP can be used as a sensing element with the merit of low cost, controllable shape, and high sensitivity. The change in shape can generate an electrical signal because of the redistribution of ions in the IL-iEAP. Prasad *et al.* [145] reported a strain sensor made of a carbon nanofiber/IL/PVDF membrane with a high gauge factor (4.08). He *et al.* [146] produced an electromechanical sensing transducer by mixing chitosan and glycerin into the electrolyte layer. The sensing output voltage of this novel IL-iEAP with graphene electrodes was 2.74–4.52 times higher than the traditional IPMC. IL-iEAP can provide high-quality feedback signals because of its electromechanical coupling properties. With the suitable design of the transducer's structure, IL-iEAP has the potential to perform dual actuation and sensing functions. However, most of the IL-iEAP device developed can only perform single function, either an actuator or a sensor, and the measurement of bending strain of the actuator requires an external sensor. Therefore, developing IL-iEAP actuator with a self-sensing function may form a new research direction to broaden its potential application [147,148]. Recently, Panwar *et al.* [35] fabricated a self-sensing electronic skin consisting of terpolymer and BMIMHS (1-butyl-3-methylimidazolium hydrogen sulfate) for a wearable energy harvesting device in which the energy was collected from human sweating, with output self-sensing voltage recorded up to 550 mV. However, it is challenging to realize real-time feedback for the deformation of IL-iEAP without external sensing equipment, especially when the sample is in a complex operating environment.

6 Future prospects

A challenge in fabricating IL-iEAPs is to obtain an electrolyte layer with environmental stability and electrode layers with excellent flexibility and electrical property simultaneously. Recently, customizing the IL-iEAP actuator or sensor by designing the material composition, morphology, and processing method can be achieved by introducing nanostructured materials. Metal electrodes with hundreds of nanometers thickness have been successfully deposited onto polymer electrolyte surfaces through physical vapor deposition. The electrodes have demonstrated good adhesion and low interfacial resistance [149]. Magnetron sputtering is another commonly used coating method for coating metal electrodes [150].

However, this layered iEAP actuator is still limited in performing bending deformation. Therefore, one of the challenging issues is how to develop IL-iEAP actuators with an ability to perform complex actuation behavior such as curling, torsion, or oscillation, through structural design. For instance, nylon fiber prepared by electrospinning with depositing PPy electrodes performed a spiral motion at ±3.5 V [151], and this EAP actuator also responds to pH or temperature change when immersed in solution and can be used to perform grasping of micro-objects. Khaldi *et al.* [152] believed that individual control of micro-size actuators can be achieved by combining laser ablation and laser etching technology to fabricate IL-iEAP. Other technologies, such as 3D printing [153], are being explored for constructing free form IL-iEAP and eEAP [154]. Furthermore, it is worth noting that IL-iEAPs with actuation and sensing properties are suitable for transparent flexible electronics such as invisible devices, tactile screens, and zoomable lenses. However, the transparency of IL-iEAP is usually limited by its multilayer structure and materials. Terasawa [85,155] developed two kinds of blue transparent IL-iEAP by spray-coating PEDOT: PSS onto PDMS/IL and cellulose/IL membranes. The highest strain can reach up to 0.9% under ±2 V voltage. Although numerous research studies have been reported on transparent flexible electrodes, it is still challenging to maintain high transparency and good interfacial bonding of the iEAP after adding the electrode layers. Therefore, dielectric elastomer actuators that do not require electrodes to be

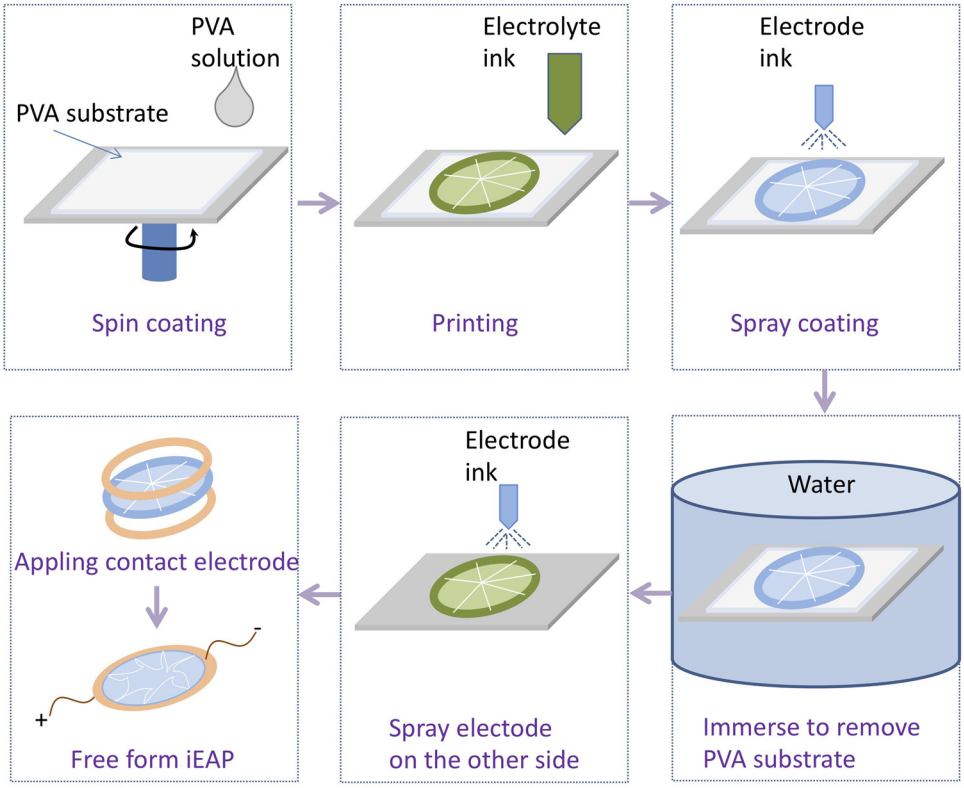

Figure 7: Strategy of fabricating free form iEAP.

completely covered usually exhibit high transparency. Combining drop-on-demand printing of electrode materials and additive manufacturing of electrolyte can be a viable method for preparing transparent iEAPs. As shown in Figure 7, it has been proposed to directly print a gradient electrolyte layer on the PVA substrate, followed by spraying the electrode on the electrolyte. After drying, the PVA substrate is removed in water. The opposite electrode is then sprayed on the other side of the electrolyte layer to obtain the free form iEAP. The driving behavior of this iEAP can be controlled by adjusting the structural parameters of the electrolyte layer during printing.

7 Conclusion

IL-iEAP shows broad application prospects in the field of biological actuators and sensors, especially the development of the self-sensing function. This article has reviewed the development history of EAPs, outlined the actuation mechanisms of three kinds of iEAPs with different electrodes, and introduced the common preparation processes for IL containing iEAPs. By analyzing the response rate and bending strain of IL-iEAP under different electrical stimulation conditions, it is suggested that an electrolyte with high ionic conductivity and electrodes with high electronic conductivity are favorable for achieving fast and large deformation of the IL-iEAP actuator. In addition, advanced fabrication technologies, such as 3D printing, have emerged as a new development trend to enhance the functionality of IL-iEAPs.

Author contributions: All authors have accepted responsibility for the entire content of this manuscript and approved its submission.

Funding information: The work described in this paper was fully supported by a grant from the Research Grants Council of the Hong Kong Special Administrative Region, China (Project No. PolyU 15200318).

Conflict of interest: The authors state no conflict of interest.

References

[1] Carrico JD, Tyler T, Leang KK. A comprehensive review of select smart polymeric and gel actuators for soft

mechatronics and robotics applications: fundamentals, freeform fabrication, and motion control. Int J Smart Nano Mater. 2017;8:144–213.
[2] Lin X, Han Q, Huang J. Effect of defects on the motion of carbon nanotube thermal actuator. Nanotechnol Rev. 2019;8:79–89.
[3] Zhan Z, Wei F, Zheng J, Yang W, Luo J, Yao L. Recent advances of light-driven micro/nanomotors: toward powerful thrust and precise control. Nanotechnol Rev. 2018;7:555–81.
[4] Lei M, Chen Z, Lu H, Yu K. Recent progress in shape memory polymer composites: methods, properties, applications and prospects. Nanotechnol Rev. 2019;8:327–51.
[5] Chang L, Liu Y, Yang Q, Yu L, Liu J, Zhu Z, et al. Ionic electro-active polymers used in bionic robots: a review. J Bionic Eng. 2018;15:765–82.
[6] Annabestani M, Fardmanesh M. Ionic electro active polymer-based soft actuators and their applications in microfluidic micropumps, microvalves, and micromixers: a review. Appl Phys., arXiv. 2019;1904:07149.
[7] Zarren G, Nisar B, Sher F. Synthesis of anthraquinone-based electroactive polymers: a critical review. Mater Today Sustain. 2019;5:100019.
[8] Kumar R, Senthamaraikannan P, Saravanakumar S, Khan A, Ganesh K, Ananth SV. Electroactive polymer composites and applications. In: Polymer Nanocomposite-Based Smart Materials. Cambridge, UK: Woodhead Publishing; 2020. p. 149–56.
[9] Kanik M, Orguc S, Varnavides G, Kim J, Benavides T, Gonzalez D, et al. Strain-programmable fiber-based artificial muscle. Science. 2019;365:145–50.
[10] Bauer S, Bauer-Gogonea S, Graz I, Kaltenbrunner M, Keplinger C, Schwödiauer R. 25th anniversary article: a soft future: from robots and sensor skin to energy harvesters. Adv Mater. 2014;26:149–62.
[11] Joyee EB, Pan Y. Multi-material additive manufacturing of functional soft robot. Procedia Manuf. 2019;34:566–73.
[12] Bauer S. Electroactive polymers for healthcare and bio-medical applications. Electroactive Polymer Actuators and Devices (EAPAD). 2017, Portland, Oregon, United States: International Society for Optics and Photonics; 25–29 March 2017. p. 1016303.
[13] Chang XL, Chee PS, Lim EH. A microreservoir-based drug delivery device using ionic polymer metal composite (IPMC) actuator. TENCON 2018–2018 IEEE Region 10 Conference. 2018, Jeju, Korea (South): IEEE; 28–31 October 2018. p. 0899–902.
[14] Bashir M, Rajendran P. A review on electroactive polymers development for aerospace applications. J Intell Mater Syst Struct. 2018;29:3681–95.
[15] Bar-Cohen Y, Anderson IA. Electroactive polymer (EAP) actuators—background review. Mech Soft Mater. 2019;1:5.
[16] Roentgen W. About the changes in shape and volume of dielectrics caused by electricity. Annu Phys Chem Ser. 1880;11:771–86.
[17] Kawai H. The piezoelectricity of poly (vinylidene fluoride). Japanese J Appl Phys. 1969;8:975.
[18] Hau S, Bruch D, Rizzello G, Motzki P, Seelecke S. Silicone based dielectric elastomer strip actuators coupled with nonlinear biasing elements for large actuation strains. Smart Mater Struct. 2018;27:074003.
[19] Bernat J, Kolota J. Adaptive observer for state and load force estimation for dielectric electro-active polymer actuator. IFAC-PapersOnLine. 2019;52:448–53.
[20] Lu F, Chen T, Xiang K, Wang Y. Ionic electro-active polymer actuator based on cobalt-containing nitrogen-doped carbon/conducting polymer soft electrode. Polym Test. 2020;84:106413.
[21] Suzumori K, Nabae H, Asaka K, Horiuchi T. Applying IPMC to soft robots. In: Electroactive Polymer Actuators and Devices (EAPAD) XXII. California, USA: SPIE; 27 April–9 May 2020. p. 113750A.
[22] Melling D, Martinez JG, Jager EW. Conjugated polymer actuators and devices: progress and opportunities. Adv Mater. 2019;31:1808210.
[23] Zhang Y-F, Du F-P, Chen L, Yeung K-W, Dong Y, Law W-C, et al. Supramolecular ionic polymer/carbon nanotube composite hydrogels with enhanced electromechanical performance. Nanotechnol Rev. 2020;9:478–88.
[24] Asaka K, Mukai K, Sugino T, Kiyohara K. Ionic electroactive polymer actuators based on nano-carbon electrodes. Polym Int. 2013;62:1263–70.
[25] Terasawa N, Asaka K. High-performance ionic and non-ionic fluoropolymer/ionic liquid (with quaternary cation and perfluoroalkyltrifluoroborate anion) gel hybrid actuators with electrochemical window of 6 V. Mater Today Proc. 2020;20:265–72.
[26] Vunder V. Modeling and characterization of back-relaxation of ionic electroactive polymer actuators, PhD thesis. Tartu, Estonia: Tartuensis University; 2016.
[27] Shanmugam SN, Punning A, Johanson U, Aabloo A. Modelling and control of self-sensing ionic electroactive polymer actuator. Electroactive Polymer Actuators and Devices (EAPAD) XXI. 2019, Denver, Colorado, USA: International Society for Optics and Photonics; 4–7 March 2019. p. 109661C.
[28] Kim O, Kim H, Choi UH, Park MJ. One-volt-driven superfast polymer actuators based on single-ion conductors. Nat Commun. 2016;7:1–8.
[29] Coles SW, Smith AM, Fedorov MV, Hausen F, Perkin S. Interfacial structure and structural forces in mixtures of ionic liquid with a polar solvent. Faraday Discuss. 2017;206:427–42.
[30] Almomani A, Hong W, Hong W, Montazami R. Influence of temperature on the electromechanical properties of ionic liquid-doped ionic polymer-metal composite actuators. Polymers. 2017;9:358.
[31] Guo D, Han Y, Huang J, Meng E, Ma L, Zhang H, et al. Hydrophilic poly (vinylidene fluoride) film with enhanced inner channels for both water-and ionic liquid-driven ion-exchange polymer metal composite actuators. ACS Appl Mater Interfaces. 2019;11:2386–97.
[32] Kim MJ, Park SW, Won J, Nah C. Effects of ionic liquids on the performance of IPMC. Electroactive Polymer Actuators and Devices (EAPAD). 2017, Portland, Oregon, United States: International Society for Optics and Photonics; 25–29 March 2017. p. 1016335.
[33] Woehling V, Nguyen GT, Plesse C, Petel Y, Dobashi Y, Madden JD, et al. Study of the piezoionic effect and influence of electrolyte in conducting polymer based soft strain sensors. Multifunct Mater. 2019;2:045002.

[34] Liu Y, Lu C, Twigg S, Ghaffari M, Lin J, Winograd N, et al. Direct observation of ion distributions near electrodes in ionic polymer actuators containing ionic liquids. Sci Rep. 2013;3:973.
[35] Panwar V, Mohanty S, Anoop G, Kumar S. Actuation and self-sensing performance of soft polymer actuator skin using polyelectrolyte attached terpolymer. Sens Actuators A Phys. 2020;315:112277.
[36] Montiel MA, Solla-Gullón J, Sanchez-Sanchez CM. Electrochemical reactivity and stability of platinum nanoparticles in imidazolium-based ionic liquids. J Solid State Electrochem. 2016;20:1043–52.
[37] MohdIsa W, Hunt A, HosseinNia SH. Sensing and self-sensing actuation methods for ionic polymer-metal composite (ipmc): a review. Sensors. 2019;19:3967.
[38] Yan X, Gang Z, Yuming Z, Zhuangzhi S. Morphology characterization and failure mechanism investigation of Ag-IPMC. Ionics. 2015;21:1089–94.
[39] Zhu Z, Bian C, Ru J, Bai W, Chen H. Rapid deformation of IPMC under a high electrical pulse stimulus inspired by action potential. Smart Mater Struct. 2018;28:01LT01.
[40] Guo D, Wang L, Wang X, Xiao Y, Wang C, Chen L, et al. PEDOT coating enhanced electromechanical performances and prolonged stable working time of IPMC actuator. Sens Actuators B Chem. 2020;305:127488.
[41] Saccardo MC, Zuquello AG, Tozzi KA, Gonçalves R, Hirano LA, Scuracchio CH. Counter-ion and humidity effects on electromechanical properties of Nafion®/Pt composites. Mater Chem Phys. 2020;244:122674.
[42] Yang L, Zhang D, Zhang X, Tian A, Ding Y. Surface roughening of Nafion membranes using different route planning for IPMCs. Int J Smart Nano Mater. 2020;36:1–12.
[43] Caponetto R, De Luca V, Graziani S, Sapuppo F. An optimized frequency-dependent multiphysics model for an ionic polymer-metal composite actuator with ethylene glycol as the solvent. Smart Mater Struct. 2013;22:125016.
[44] Shen Q, Wang T, Liang J, Wen L. Hydrodynamic performance of a biomimetic robotic swimmer actuated by ionic polymer-metal composite. Smart Mater Struct. 2013;22:075035.
[45] Jung Y, Kim SJ, Kim KJ, Lee DY. Characteristics of ionic polymer-metal composite with chemically doped TiO_2 particles. Smart Mater Struct. 2011;20:124004.
[46] Park M, Yoo S, Bae Y, Kim S, Jeon M. Enhanced Stability and driving performance of GO-Ag-NW-based ionic electroactive polymer actuators with triton X-100-PEDOT: PSS nanofibrils. Polymers. 2019;11:906.
[47] Yu C-Y, Zhang Y-W, Su G-DJ. Reliability tests of ionic polymer metallic composites in dry air for actuator applications. Sens Actuators A Phys. 2015;232:183–9.
[48] Tsuzuki S, Tokuda H, Hayamizu K, Watanabe M. Magnitude and directionality of interaction in ion pairs of ionic liquids: relationship with ionic conductivity. J Phys Chem B. 2005;109:16474–81.
[49] Liu Y, Liu S, Lin J, Wang D, Jain V, Montazami R, et al. Ion transport and storage of ionic liquids in ionic polymer conductor network composites. Appl Phys Lett. 2010;96:223503.
[50] Imaizumi S, Kato Y, Kokubo H, Watanabe M. Driving mechanisms of ionic polymer actuators having electric double layer capacitor structures. J Phys Chem B. 2012;116:5080–9.
[51] Terasawa N, Asaka K. High performance polymer actuators based on single-walled carbon nanotube gel using ionic liquid with quaternary ammonium or phosphonium cations and with electrochemical window of 6 V. Sens Actuators B Chem. 2014;193:851–6.
[52] Ishii S, Kokubo H, Hashimoto K, Imaizumi S, Watanabe M. Tetra-PEG network containing ionic liquid synthesized via Michael addition reaction and its application to polymer actuator. Macromolecules. 2017;50:2906–15.
[53] Bennett MD, Leo DJ. Ionic liquids as stable solvents for ionic polymer transducers. Sens Actuators A Phys. 2004;115:79–90.
[54] Zhao P, Tang Q, Zhao X, Tong Y, Liu Y. Highly stable and flexible transparent conductive polymer electrode patterns for large-scale organic transistors. J Colloid Interface Sci. 2018;520:58–63.
[55] Vidal F, Plesse C, Palaprat G, Kheddar A, Citerin J, Teyssié D, et al. Conducting IPN actuators: from polymer chemistry to actuator with linear actuation. Synth Met. 2006;156:1299–304.
[56] McInnis M, Zhai L. Conjugated polymer/carbon nanotube composites. Rev Nanosci Nanotechnol. 2012;1:119–41.
[57] Yang C, Zhang P, Nautiyal A, Li S, Liu N, Yin J, et al. Tunable three-dimensional nanostructured conductive polymer hydrogels for energy-storage applications. ACS Appl Mater Interfaces. 2019;11:4258–67.
[58] Kaneto K, Kaneko M, Min Y, MacDiarmid AG. "Artificial muscle": electromechanical actuators using polyaniline films. Synth Met. 1995;71:2211–2.
[59] Otero TF, Sansieña JM. Soft and wet conducting polymers for artificial muscles. Adv Mater. 1998;10:491–4.
[60] Zhou D, Spinks GM, Wallace GG, Tiyapiboonchaiya C, MacFarlane DR, Forsyth M, et al. Solid state actuators based on polypyrrole and polymer-in-ionic liquid electrolytes. Electrochim Acta. 2003;48:2355–9.
[61] Otero T, Martinez J, Arias-Pardilla J. Biomimetic electrochemistry from conducting polymers. A review: artificial muscles, smart membranes, smart drug delivery and computer/neuron interfaces. Electrochim Acta. 2012;84:112–28.
[62] Carpi F, Smela E. Biomedical applications of electroactive polymer actuators. UK: John Wiley & Sons; 2009.
[63] Elhi F, Priks H, Rinne P, Kaldalu N, Žusinaite E, Johanson U, et al. Electromechanically active polymer actuators based on biofriendly choline ionic liquids. Smart Mater Struct. 2020;29:055021.
[64] Kesküla A, Peikolainen A-L, Kiefer R, Tamm T. Consistent response from conducting polymer actuators: potential window and embedded charges to avoid mixed ion transport. Synth Met. 2020;268:116502.
[65] Lee J, Aida T. "Bucky gels" for tailoring electroactive materials and devices: the composites of carbon materials with ionic liquids. ChemComm. 2011;47:6757–62.
[66] Morozov O, Shachneva S, Bulgakov B, Babkin A, Kepman A. Effect of different pore-forming additives on the formation of pvdf microporous membranes for bucky–gel actuator. Eurasian Chem-Technol J. 2020;22:107–15.
[67] Fukushima T, Kosaka A, Ishimura Y, Yamamoto T, Takigawa T, Ishii N, et al. Molecular ordering of organic molten salts triggered by single-walled carbon nanotubes. Science. 2003;300:2072–4.

[68] Ventrapragada LK, Creager SE, Rao AM, Podila R. Carbon nanotubes coated paper as current collectors for secondary Li-ion batteries. Nanotechnol Rev. 2019;8:18–23.
[69] Kim SG, You NH, Lee W, Hwang JY, Kim MJ, Hui D, et al. Effects of the functionalized graphene oxide on the oxygen barrier and mechanical properties of layer-by-layer assembled films. Compos B Eng. 2016;92:307–14.
[70] Naghib SM, Behzad F, Rahmanian M, Zare Y, Rhee KY. A highly sensitive biosensor based on methacrylated graphene oxide-grafted polyaniline for ascorbic acid determination. Nanotechnol Rev. 2020;9:760–7.
[71] Yang Q, Liu L, Hui D, Chipara M. Microstructure, electrical conductivity and microwave absorption properties of γ-FeNi decorated carbon nanotube composites. Compos B Eng. 2016;87:256–62.
[72] Gao M, Zheng F, Xu J, Zhang S, Bhosale SS, Gu J, et al. Surface modification of nano-sized carbon black for reinforcement of rubber. Nanotechnol Rev. 2019;8:405–14.
[73] Li Z, Xu K, Pan Y. Recent development of supercapacitor electrode based on carbon materials. Nanotechnol Rev. 2019;8:35–49.
[74] Pan Y, Xu K, Wu C. Recent progress in supercapacitors based on the advanced carbon electrodes. Nanotechnol Rev. 2019;8:299–314.
[75] Dassan EGB, Ab Rahman AA, Abidin MSZ, Akil HM. Carbon nanotube-reinforced polymer composite for electromagnetic interference application: a review. Nanotechnol Rev. 2020;9:768–88.
[76] Yeung K-W, Dong Y, Chen L, Tang C-Y, Law W-C, Tsui GC-P, et al. Printability of photo-sensitive nanocomposites using two-photon polymerization. Nanotechnol Rev. 2020;9:418–25.
[77] Baughman RH, Cui C, Zakhidov AA, Iqbal Z, Barisci JN, Spinks GM, et al. Carbon nanotube actuators. Science. 1999;284:1340–4.
[78] Hughes M, Spinks GM. Multiwalled carbon nanotube actuators. Adv Mater. 2005;17:443–6.
[79] Mirfakhrai T, Kozlov M, Fang S, Zhang M, Baughman RH, Madden JD. Carbon nanotube yarns: sensors, actuators, and current carriers. Electroactive Polymer Actuators and Devices (EAPAD). 2008, San Diego, California, USA: International Society for Optics and Photonics; 10–13 March 2008. p. 692708.
[80] Fukushima T, Asaka K, Kosaka A, Aida T. Fully plastic actuator through layer-by-layer casting with ionic-liquid-based bucky gel. Angew Chem Int Ed. 2005;44:2410–3.
[81] Takeuchi I, Asaka K, Kiyohara K, Sugino T, Terasawa N, Mukai K, et al. Electromechanical behavior of fully plastic actuators based on bucky gel containing various internal ionic liquids. Electrochim Acta. 2009;54:1762–8.
[82] Mukai K, Asaka K, Kiyohara K, Sugino T, Takeuchi I, Fukushima T, et al. High performance fully plastic actuator based on ionic-liquid-based bucky gel. Electrochim Acta. 2008;53:5555–62.
[83] Naficy S, Stoboi N, Whitten PG, Spinks GM, Wallace GG. Evaluation of encapsulating coatings on the performance of polypyrrole actuators. Smart Mater Struct. 2013;22:075005.
[84] Khmelnitskiy I, Aivazyan V, Alekseev N, Broyko A, Golubkov V, Testov D, et al. Producing and investigation of PEDOT films as electrodes of ionic electroactive actuators. J Phys Conf Ser. 2019;012033.
[85] Terasawa N. High-performance transparent actuator made from Poly (dimethylsiloxane)/Ionic liquid gel. Sens Actuators B Chem. 2018;257:815–9.
[86] Kim SS, Jeon JH, Kee CD, Oh IK. Electro-active hybrid actuators based on freeze-dried bacterial cellulose and PEDOT: PSS. Smart Mater Struct. 2013;22:085026.
[87] Hu F, Xue Y, Xu J, Lu B. PEDOT-based conducting polymer actuators. Front Robot AI. 2019;6:17.
[88] Kotal M, Kim J, Kim KJ, Oh IK. Sulfur and nitrogen co-doped graphene electrodes for high-performance ionic artificial muscles. Adv Mater. 2016;28:1610–5.
[89] Morozov O, Shachneva S, Kepman A. Microporous PVDF ionic membranes for actuator applications prepared with imidazole-based poly (ionic) liquid as a pore forming material. IOP Conf Ser Mater Sci Eng. 2019;17:012060.
[90] Lee JW, Yoo YT. Anion effects in imidazolium ionic liquids on the performance of IPMCs. Sens Actuators B Chem. 2009;137:539–46.
[91] Doyle M, Choi SK, Proulx G. High-temperature proton conducting membranes based on perfluorinated ionomer membrane-ionic liquid composites. J Electrochem Soc. 2000;147:34.
[92] Akle BJ, Bennett MD, Leo DJ. High-strain ionomeric-ionic liquid electroactive actuators. Sens Actuators A Phys. 2006;126:173–81.
[93] Wu Y, Alici G, Spinks GM, Wallace G. Fast trilayer polypyrrole bending actuators for high speed applications. Synth Met. 2006;156:1017–22.
[94] Khmelnitskiy IK, Aivazyan VM, Andryukhin KA, Lagosh AV, Kalyonov VE. PEDOT and PANI electrodes for IP^{2}C actuators. 2019 IEEE Conference of Russian Young Researchers in Electrical and Electronic Engineering (ElConRus). 2019, Moscow and St. Petersburg, Russia: IEEE; 28–31 January 2019. p. 815–8.
[95] Li Y, Qian R. Stability of conducting polymers from the electrochemical point of view. Synth Met. 1993;53:149–54.
[96] Lin J, Liu Y, Zhang Q. Charge dynamics and bending actuation in Aquivion membrane swelled with ionic liquids. Polymer. 2011;52:540–6.
[97] Kwon KS, Ng TN. Improving electroactive polymer actuator by tuning ionic liquid concentration. Org Electron. 2014;15:294–8.
[98] Mukai K, Asaka K, Sugino T, Kiyohara K, Takeuchi I, Terasawa N, et al. Highly conductive sheets from millimeter-long single-walled carbon nanotubes and ionic liquids: application to fast-moving, low-voltage electromechanical actuators operable in air. Adv Mater. 2009;21:1582–5.
[99] Asai H, Okumura T, Sakamoto H, Nakane K. Effect of polymer type on the performance of a nanofiber mat actuator. Polym J. 2019;51:523–8.
[100] Huang D, Goh T, Kong J, Zheng Y, Zhao S, Xu Z, et al. Perovskite solar cells with a DMSO-treated PEDOT: PSS hole transport layer exhibit higher photovoltaic performance and enhanced durability. Nanoscale. 2017;9:4236–43.
[101] Simaite A, Tondu B, Souères P, Bergaud C. Hybrid PVDF/PVDF-graft-PEGMA membranes for improved interface strength and lifetime of PEDOT: PSS/PVDF/ionic liquid actuators. ACS Appl Mater Interfaces. 2015;7:19966–77.

[102] Põldsalu I, Rohtlaid K, Nguyen TMG, Plesse C, Vidal F, Khorram MS, et al. Thin ink-jet printed trilayer actuators composed of PEDOT: PSS on interpenetrating polymer networks. Sens Actuators B Chem. 2018;258:1072–9.
[103] Park M, Kim J, Song H, Kim S, Jeon M. Fast and stable ionic electroactive polymer actuators with PEDOT: PSS/(Graphene-Ag-Nanowires) nanocomposite electrodes. Sensors. 2018;18:3126.
[104] Zhao G, Sun Z, Wang J, Xu Y, Muhammad F. Development of biocompatible polymer actuator consisting of biopolymer chitosan, carbon nanotubes, and an ionic liquid, Poly. Compos. 2017;38:1609–15.
[105] Noda A, Hayamizu K, Watanabe M. Pulsed-gradient spin–echo 1H and 19F NMR ionic diffusion coefficient, viscosity, and ionic conductivity of non-chloroaluminate room-temperature ionic liquids. J Phys Chem B. 2001;105:4603–10.
[106] Tang Y, Xue Z, Xie X, Zhou X. Ionic polymer-metal composite actuator based on sulfonated poly (ether ether ketone) with different degrees of sulfonation. Sens Actuators A Phys. 2016;238:167–76.
[107] Lagosh AV, Broyko AP, Kalyonov VE, Khmelnitskiy IK, Luchinin VV. Modeling of IPMC actuator 2017 IEEE conference of Russian young researchers in electrical and electronic engineering (EIConRus). IEEE; 2017. p. 916–8.
[108] Mejri R, Dias J, Hentati SB, Botelho G, Esperança J, Costa C, et al. Imidazolium-based ionic liquid type dependence of the bending response of polymer actuators. Eur Polym J. 2016;85:445–51.
[109] Asaka K, Fujiwara N, Oguro K, Onishi K, Sewa S. State of water and ionic conductivity of solid polymer electrolyte membranes in relation to polymer actuators. J Electroanal Chem. 2001;505:24–32.
[110] Nemat-Nasser S. Micromechanics of actuation of ionic polymer-metal composites. J Appl Phys. 2002;92:2899–915.
[111] Akle BJ, Hickner M, Leo DJ, McGrath JE. Electroactive polymers based on novel ionomers. ASME International Mechanical Engineering Congress and Exposition; 2003. p. 445–52.
[112] Liu Y, Ghaffari M, Zhao R, Lin J-H, Lin M, Zhang Q. Enhanced electromechanical response of ionic polymer actuators by improving mechanical coupling between ions and polymer matrix. Macromolecules. 2012;45:5128–33.
[113] Alici G, Mui B, Cook C. Bending modeling and its experimental verification for conducting polymer actuators dedicated to manipulation applications. Sens Actuators A Phys. 2006;126:396–404.
[114] Ebadi SV, Semnani D, Fashandi H, Rezaei B. Synthesis and characterization of a novel polyurethane/polypyrrole-p-toluenesulfonate (PU/PPy-pTS) electroactive nanofibrous bending actuator. Polym Adv Technol. 2019;30:2261–74.
[115] Sangian D, Zheng W, Spinks GM. Optimization of the sequential polymerization synthesis method for polypyrrole films. Synth Met. 2014;189:53–6.
[116] Cui X, Martin DC. Electrochemical deposition and characterization of poly (3, 4-ethylenedioxythiophene) on neural microelectrode arrays. Sens Actuators B Chem. 2003;89:92–102.
[117] Kim N, Kee S, Lee SH, Lee BH, Kahng YH, Jo YR, et al. Highly conductive PEDOT: PSS nanofibrils induced by solution-processed crystallization. Adv Mater. 2014;26:2268–72.
[118] Rasouli H, Naji L, Hosseini MG. The influence of electrodeposited conducting polymer electrode structure on the actuation performance of muscle-like ionic actuators. Sens Actuators A Phys. 2018;279:204–15.
[119] Khan A, Alamry KA, Jain RK. Polypyrrole nanoparticles-based soft actuator for artificial muscle applications. RSC Adv. 2019;9:39721–34.
[120] Zainudeen UL, Careem MA, Skaarup S. PEDOT and PPy conducting polymer bilayer and trilayer actuators. Sens Actuators B Chem. 2008;134:467–70.
[121] Terasawa N, Asaka K. High-performance PEDOT: PSS/single-walled carbon nanotube/ionic liquid actuators combining electrostatic double-layer and faradaic capacitors. Langmuir. 2016;32:7210–8.
[122] Teo MY, Kim N, Kee S, Kim BS, Kim G, Hong S, et al. Highly stretchable and highly conductive PEDOT: PSS/ionic liquid composite transparent electrodes for solution-processed stretchable electronics. ACS Appl Mater Interfaces. 2017;9:819–26.
[123] Wang D, Lu C, Zhao J, Han S, Wu M, Chen W. High energy conversion efficiency conducting polymer actuators based on PEDOT: PSS/MWCNTs composite electrode. RSC Adv. 2017;7:31264–71.
[124] Takeuchi I, Asaka K, Kiyohara K, Sugino T, Mukai K, Randriamahazaka H. Electrochemical impedance spectroscopy and electromechanical behavior of bucky-gel actuators containing ionic liquids. J Phys Chem C. 2010;114:14627–34.
[125] Randriamahazaka H, Asaka K. Electromechanical analysis by means of complex capacitance of bucky-gel actuators based on single-walled carbon nanotubes and an ionic liquid. J Phys Chem C. 2010;114:17982–8.
[126] Biso M, Ansaldo A, Futaba DN, Hata K, Ricci D. Cross-linking super-growth carbon nanotubes to boost the performance of bucky gel actuators. Carbon. 2011;49:2253–7.
[127] Li J, Ma W, Song L, Niu Z, Cai L, Zeng Q, et al. Superfast-response and ultrahigh-power-density electromechanical actuators based on hierarchal carbon nanotube electrodes and chitosan. Nano Lett. 2011;11:4636–41.
[128] Terasawa N, Ono N, Mukai K, Koga T, Higashi N, Asaka K. A multi-walled carbon nanotube/polymer actuator that surpasses the performance of a single-walled carbon nanotube/polymer actuator. Carbon. 2012;50:311–20.
[129] Torop J, Palmre V, Arulepp M, Sugino T, Asaka K, Aabloo A. Flexible supercapacitor-like actuator with carbide-derived carbon electrodes. Carbon. 2011;49:3113–9.
[130] Terasawa N, Asaka K. High-performance graphene oxide/vapor-grown carbon fiber composite polymer actuator. Sens Actuators B Chem. 2018;255:2829–37.
[131] Terasawa N, Asaka K. High-performance cellulose nanofibers, single-walled carbon nanotubes and ionic liquid actuators with a poly (vinylidene fluoride-co-hexafluoropropylene)/ionic liquid gel electrolyte layer. RSC Adv. 2019;9:8215–21.
[132] Wu G, Li G, Lan T, Hu Y, Li Q, Zhang T, et al. An interface nanostructured array guided high performance electrochemical actuator. J Mater Chem A. 2014;2:16836–41.
[133] Terasawa N. High-performance ionic and non-ionic fluoropolymer/ionic liquid gel hybrid actuators based on single-walled carbon nanotubes. RSC Adv. 2017;7:2443–9.

[134] Chen Z, Um TI, Bart-Smith H. Bio-inspired robotic manta ray powered by ionic polymer-metal composite artificial muscles. Int J Smart Nano Mater. 2012;3:296–308.
[135] Guo D-J, Liu R, Cheng Y, Zhang H, Zhou L-M, Fang S-M, et al. Reverse adhesion of a gecko-inspired synthetic adhesive switched by an ion-exchange polymer-metal composite actuator. ACS Appl Mater Interfaces. 2015;7:5480–7.
[136] Must I, Kaasik F, Poldsalu I, Mihkels L, Johanson U, Punning A, et al. Ionic and capacitive artificial muscle for biomimetic soft robotics. Adv Eng Mater. 2015;17:84–94.
[137] He Q, Liu Z, Yin G, Yue Y, Yu M, Li H, et al. The highly stable air-operating ionic polymer metal composite actuator with consecutive channels and its potential application in soft gripper. Smart Mater Struct. 2020;29:045013.
[138] Fukuda K, Sekitani T, Zschieschang U, Klauk H, Kuribara K, Yokota T, et al. A 4 V operation, flexible braille display using organic transistors, carbon nanotube actuators, and organic static random-access memory. Adv Funct Mater. 2011;21:4019–27.
[139] Ikushima K, John S, Ono A, Nagamitsu S. PEDOT/PSS bending actuators for autofocus micro lens applications. Synth Met. 2010;160:1877–83.
[140] Ghamsari K, Zegeye A, Jin E, Woldesenbet YE. Application of bucky gel in fabrication of a low-voltage rapid microvalve for flow regulation. ACS Appl Mater Interfaces. 2013;5:5408–12.
[141] Balint R, Cassidy NJ, Cartmell SH. Conductive polymers: towards a smart biomaterial for tissue engineering. Acta Biomater. 2014;10:2341–53.
[142] Egorova KS, Ananikov VP. Toxicity of ionic liquids: eco (cyto) activity as complicated, but unavoidable parameter for task-specific optimization. ChemSusChem. 2014;7:336–60.
[143] Elhi F, Karu K, Rinne P, Nadel K-A, Järvekülg M, Aabloo A, et al. Understanding the behavior of fully non-toxic poly-pyrrole-gelatin and polypyrrole-PVdF soft actuators with choline ionic liquids. Actuators. 2020;40.
[144] Rinne P, Põldsalu I, Johanson U, Tamm T, Põhako-Esko K, Punning A, et al. Encapsulation of ionic electromechanically active polymer actuators. Smart Mater Struct. 2019;28:074002.
[145] Prasad B, Gill FS, Panwar V, Anoop G. Development of strain sensor using conductive poly (vinylidene fluoride) (PVDF) nanocomposite membrane reinforced with ionic liquid (IL) & carbon nanofiber (CNF). Compos B Eng. 2019;173:106990.
[146] He Q, Vokoun D, Stalbaum T, Kim KJ, Fedorchenko AI, Zhou X, et al. Mechanoelectric transduction of ionic polymer-graphene composite sensor with ionic liquid as electrolyte. Sens Actuators A Phys. 2019;286:68–77.
[147] Kruusamäe K, Punning A, Aabloo A, Asaka K. Self-sensing ionic polymer actuators: a review. Actuators. 2015;4:17–38.
[148] Liu Y, Zhong Y, Wang C. Recent advances in self-actuation and self-sensing materials: state of the art and future perspectives. Talanta. 2020;212:120808.
[149] Kim J. Multifunctional smart biopolymer composites as actuators. In: Biopolymer Composites in Electronics. Amsterdam, Netherlands: Elsevier; 2017. p. 311–31.
[150] Correia D, Barbosa J, Costa C, Reis P, Esperança J, de Zea Bermudez V, et al. Ionic liquid cation size-dependent electromechanical response of ionic liquid/poly (vinylidene fluoride)-based soft actuators. J Phys Chem C. 2019;123:12744–52.
[151] Beregoi M, Evanghelidis A, Diculescu VC, Iovu H, Enculescu I. Polypyrrole actuator based on electrospun microribbons. ACS Appl Mater Interfaces. 2017;9:38068–75.
[152] Khaldi A, Maziz A, Alici G, Spinks GM, Jager EW. Bottom-up microfabrication process for individually controlled conjugated polymer actuators. Sens Actuators B Chem. 2016;230:818–24.
[153] Carrico JD, Kim KJ, Leang KK. 3D-printed ionic polymer-metal composite soft crawling robot. 2017 IEEE International Conference on Robotics and Automation (ICRA). 2017, Marina Bay Sands, Singapore: IEEE; 29 May–3 June 2017. p. 4313–20.
[154] Acome E, Mitchell S, Morrissey T, Emmett M, Benjamin C, King M, et al. Hydraulically amplified self-healing electrostatic actuators with muscle-like performance. Science. 2018;359:61–5.
[155] Terasawa N. Self-standing high-performance transparent actuator based on poly (dimethylsiloxane)/TEMPO-oxidized cellulose nanofibers/ionic liquid gel. Langmuir. 2020;36(22):6154–9.